J. Build. Mater. Struct. (2023) 10: 78-90 ***Original Article***
DOI : 10.34118/jbms.v10i2.3637

Optimizing Self-Compacting Concrete through the Incorporation of Calcined Mud at 850°C

Mohamed Krachaï Rachida [1,2], Bouabdallah Moulaï Abdellah [3,4,*]

1 L.S.T.E Laboratory; Department of Civil Engineering, Mustapha Stambouli University of Mascara, Algeria.
2 Laboratoire de génie civil et environnement, LGCE, Sidi Bel Abbes, Algeria.
3,* Department of Civil Engineering, National Polytechnic School of Oran, Algeria.
4 LCTC, Laboratoire de Contrôle Technique de la Construction, Oran, Algeria.
* Corresponding Author: m-a.bouabdallah@enp-oran.dz & rm.kirachai@univ-mascara.dz

Received: 17-11-2023 **Accepted: 20-12-2023**

Abstract. The quantity of mud increases annually at dam sites, thereby reducing their storage capacity. To extend the lifespan of these structures, dam dredging is an essential solution. However, the extraction of enormous amounts of mud through the dam's bottom outlets, which remain unused, currently poses an environmental problem.

The primary objective of this research is to study the influence of mud, after thermal treatment at 850°C, added as an additive on the behavior of self-compacting concrete (SCC).

The first section of this article aims to detail the steps and essential processes for obtaining high-quality self-compacting concrete, incorporating calcined mud as an additive while adhering to current standards. The second part presents results related to mechanical compressive strength and split tensile strength concerning age.

Key words: Self-compacting concrete, The calcined mud, Fresh state test, Compressive Strength, Ultrasonic pulse velocity testing, Thermal treatment, Correlation (Rc/UVP).

1. Introduction

The silting of dams is becoming increasingly worrisome and frequent. The water volume in dams is severely threatened by mud deposits, estimated at 50 million cubic meters per year in Algeria (Benasla et al., 2015a; Bensafia & Remini, 2016; Remimi & Hallouche, 2005; Remini, 2006). However, in the face of the significant amount of mud discharged downstream from the dam, serious environmental problems have arisen (Benasla et al., 2015b).

It would be more judicious to contemplate a rational use of the mud, which can be valorized in the field of construction materials, particularly ceramics (Junakova & Junak, 2017; Mezencevova et al., 2012). As an alternative means of disposal, it is proposed to use these sludges rich in alumina and silica as a substitute for traditional pozzolans used in the commercial production of Portland cement. The mud can be employed as active additions to prepare composite cements with suitable properties (Labiod et al., 2004; Rodríguez et al., 2013).

The mud should now be considered as a beneficial product rather than a mere discharge whose storage difficulties posed an environmental problem. The dredged mud can be used based on the nature and size of sediment particles, and the energy required for cement manufacturing and grinding is higher, thus more expensive, than that needed for mud calcination (Remini, 2006).

Currently, there are several articles focusing on the valorization of mud (De Gregorio et al., 2023; Gázquez et al., 2011; Li et al., 2022; Mezencevova et al., 2012). These publications address various aspects of this issue, including calcination techniques, methods for sediment recovery, and potential applications in the construction industry. Researchers are also exploring the environmental challenges associated with sediment management and seeking innovative solutions to minimize adverse effects on aquatic ecosystems. This research update highlights the ongoing importance of finding sustainable and economically viable ways to valorize mud while contributing to environmental preservation.

Numerous research efforts have been undertaken to explore the use of calcined mud in concrete production, with the goal of developing economical and practical formulations. These studies aim to substitute up to 30% of the cement with these sediments after calcination at 750°C to activate them. Tests have been conducted to assess the quality of these concretes in both the fresh and hardened states (Safer et al., 2017).

Some have chosen to operate at temperatures of 750, 850, and 950°C (Laoufi et al., 2016), while others have preferred lower temperatures, such as 105°C (Benasla et al., 2015a). The calcination processes have varied durations, adjusted based on the specific goals of each research endeavor.

Trials in both the fresh and hardened states are crucial in research on the formulation of self-compacting concrete (Mohammed Krachaï & Bouabdallah, 2020; Safer et al., 2017). In the fresh state, these trials ensure the quality of preparation and the suitability of concrete workability. In the hardened state, these trials assess strength, durability, and other mechanical characteristics, ensuring the material's robustness to withstand structural loads and environmental conditions.

Based on the presented studies, it can be concluded that the valorization of mud remains a current research topic contributing to environmental preservation. Moreover, dam mud can be utilized as an additive in self-compacting concrete (SCC) with prior thermal treatment. The objective of this study is to demonstrate that dam mud can be used as an effective additive in self-compacting concrete (SCC). To achieve this, we conducted eight series of self-compacting concrete formulations by replacing various percentages of cement with dam mud, while comparing with other filling materials such as pozzolan and silica fume, and using class 52.5 Portland cement as a binder.

The remainder of this article is structured as follows: The second section describes sample preparation, the experimental setup, and presents the results of all experimental tests on fresh state self-compacting concrete. The third section presents the results of hardened state experimental tests (including destructive and non-destructive tests) and provides an in-depth analysis. Finally, the last section presents the conclusions of this research.

2. Experimental study

2.1. Used materials

A single type of cement, CEM II/A-L 52.5N NA 442, was used for the various concrete compositions. This is a high-strength white cement, obtained by grinding white clinker.

Table 1. Technical data for the chemical analysis of CEM II/A-L 52.5N NA 442 cement

Properties	Values
Loss on ignition (%), (NA 5042)	6.0 ± 2
Sulfate content SO3 (%)	2.5 ± 0.5
Magnesium oxide content MgO (%)	17 ± 0.5
Chloride content (%), (NA 5042)	0.02 ± 0.09

Table 2. Hypothetical composition of clinker (Bogue) for CEM II/A-L 52.5N NA 442 cement

Clinker Components	Percentage
Tricalcium silicate (C_3S)	55 ± 3
Tricalcium aluminate (C_3A)	9 ± 1

Table 3. Compression Strength of CEM II/A-L 52.5N cement NA 442

Age	Strength (MPa)
02 days	≥ 20
28 days	≥ 52.5

Table 4. Physical properties of CEM II/A-L 52.5N NA 442 cement

Properties	Values
Normal consistency of cement paste (%)	28 ± 3
Fineness by Blaine method (cm^2/g) (NA 231)	4300-5200
Shrinkage at 28 days (µm/m)	< 1000
Expansion (mm)	≤ 3

Table 5. Setting Time at 20°C (NA 230) for CEM II/A-L 52.5N cement NA 442

Setting Time	Values
Initial Setting (min)	160 ± 40
Final Setting (min)	250 ± 40

The aggregates are sourced from a specific region in the municipality of Sidi Ali Benyoub, Sidi Bel Abbés. To ensure optimal flow of self-compacting concrete, regardless of the reinforcement density, it is crucial to use aggregates with a small diameter, typically less than 20 mm. In our mixture, we incorporated two types of sand: the first one, a sand of fraction 0/1 representing fine silica sand, and the second one, a sand of fraction 0/3. The data related to the physical characterization of the aggregates used are presented in Table 6. Figure 01 illustrates the results of the particle size analysis that enabled us to obtain the granulometric curve of the mixture used in our study.

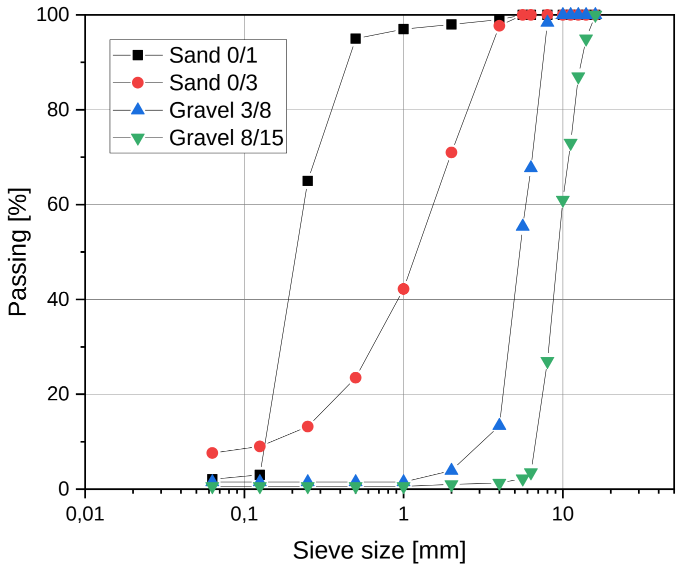

Fig 1. Particle size of the used aggregates.

Table 6. Summary of the physical characteristics of the aggregates used

Characteristics	Sand 0/1	Sand 0/3	Gravel 3/8	Gravel 8/15
Absolute Volume Mass (g/cm^3)	2.62	2.58	2.68	2.68
Apparent Volume Mass (g/cm^3)	1.45	1.62	1.37	1.43
Sand Equivalent	70			
Methylene Blue	0.75	1.5		
Water Absorption Coefficient %	0.2	1.4	0.9	0.9
Water Content (%)	3.10	1.1	0	0.70
Fine Content (%)	2.13	7.64	2	0.60
Fineness Modulus	1.42	3.43	0.60	
Los Angeles			24.70	24.70
Flakiness Index			17.20	15.00

2.2. *Additions*

Self-compacting concrete is characterized by a significant paste volume due to a higher quantity of contents compared to traditional vibrated concrete.
In our study, we used four types of fillers: limestone filler, calcined mud from the Bouhanifia dam, natural pozzolana from the Beni-saf region, and silica fume.

2.2.1. *Natural Pozzolana*

It is a natural pozzolana of volcanic origin extracted from the volcanic deposit in the Beni-Saf region (western Algeria). This pozzolana is supplied in the form of crushed rocks, such as pumice stone and scoria (Figure 2). To use it as a substitute in the composition of SCC, we first subjected it to drying at 105°C to eliminate any potential moisture and facilitate grinding. Subsequently, we thoroughly ground it and sieved it through an 80 µm sieve (Tables 7 and 8).

Fig 2. Natural Pozzolana Used, (a) before grinding, (b) after grinding

Table 7. Summary table of the chemical characteristics of natural pozzolana

Composition	SiO_2	Al_2O3	CaO	Fe_2O_3	MgO	SO_3	Cl	Na_2O_3	K_2O	LoI
Pouzzolane [%]	47.56	16.68	9.24	9.57	3.64	0.26	0.01	1.65	0.67	3.80

Table 8. Summary table of the physical characteristics of natural pozzolana

Absolute Volume Mass (g/cm^3)	2.51
Apparent Volume Mass (g/cm^3)	1.14

2.2.2. *Calcined Mud*

The entire quantity of mud used is extracted from the downstream disposal area of the Bouhanifia dam. The chemical composition of the mud suggests the transformation of stable clay structures into amorphous structures. This transformation ensures the pozzolanic reactivity sought for the intended substitution.

2.2.3. *Preparation of Calcined Mud*

The extracted mud undergoes appropriate preparation through the following process:

- Drying: The mud is initially dried in an oven at 105°C.
- Crushing: The dried mud is crushed to facilitate grinding.
- Grinding: The crushed mud undergoes electric grinding.
- Sieving: The ground mud is dry sieved through an 80 µm sieve.
- Calcination: This involves a thermal treatment performed on the prepared mud through heating at 850°C.

2.3. Thermal Treatment of the Mud

The firing rate must be set at 5 °C/min to avoid thermal shocks. Subsequently, the firing temperature, set at (850 °C ± 5), is maintained constant for 4 hours to obtain the final product, namely the calcined sludge. The latter should be stored away from air and moisture, in airtight bags (see Figures 3 and 4).

Furthermore, the choice of temperature was made based on previous research (Laoufi et al., 2016), where it is explained that the sludge, when fired at 850 °C, exhibits chemical characteristics closer to those of an active pozzolan. In other words, the three main oxides, namely (SiO_2) + (Al_2O_3) + (Fe_2O_3), surpass the 70% threshold. Thus, it can be concluded that the sludge samples, calcined at 850 °C, have values close to the 70% limit and can therefore be considered active.

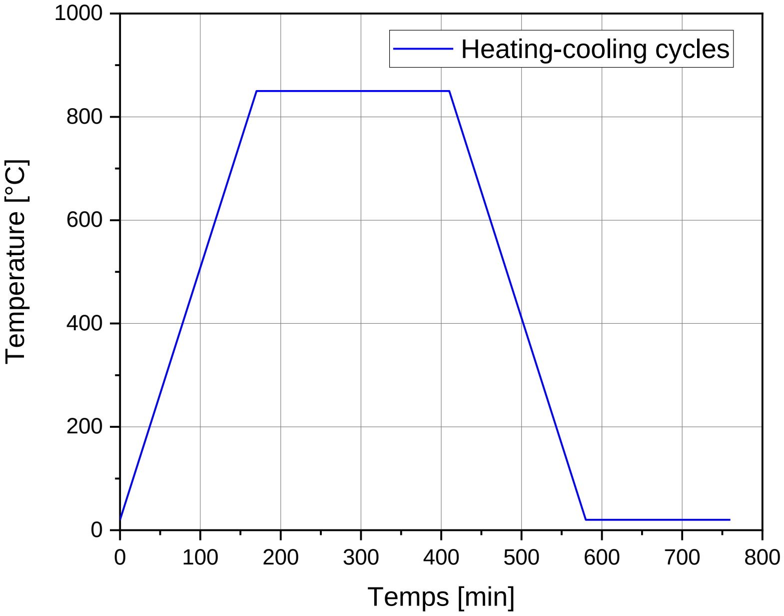

Fig 3. Heating-cooling cycles of the mud at 850°C.

Fig 4. The mud before and after calcination

The chemical and physical characteristics of the mud after calcination are presented in tables 9 and 10.

Table 9. Chemical characteristics of the mud before and after calcination.

Oxides	Raw Mud (%)	Calcined Mud (%)	Recommended Limits (%) (AFNOR, 1983)
Si O_2	46.58	57.45	35 - 85
AL_2O_3	11.89	11.23	9 - 25
CaO	11.67	13.35	0 - 25
MgO	1.36	2.65	0 - 5
Na_2O	0.88	0.95	0.1-1
Fe_2O_3	4.53	4.27	3 - 9
SO_3	1.02	0.98	0 - 3
TiO_2	0.3	0.55	0.3 - 2
K_2O	1.65	2.64	1 - 5
LoI	11.45	10.60	13

Table 10. Physical characteristics of the mud.

Bulk density (g/cm^3)	2.5
Apparent density (g/cm^3)	1.11

The limestone fillers come from a quarry located in the region of the municipality of Sidi Ali Benyoub, Sidi Bel Abbès, as shown in Figure 5.

Fig 5. Crushed limestone fillers.

Table 11. Chemical characteristics of crushed limestone fillers.

Oxides	Limestone Fillers (%)
Si O_2	11.32
AL_2O_3	0.41
CaO	53.16
MgO	0.28
Fe_2O_3	0.88
SO_3	0
LoI	21.45

Table 12. Summary of physical characteristics

Characteristics of Limestone Fillers	
Bulk density (g/cm^3)	2.47
Apparent density (g/cm^3)	1.07

2.3.1. Silica Fume

Silica fume is composed of spherical particles of amorphous SiO2, representing between 93 and 98% of its composition, with dimensions on the order of tens of microns. Its specific surface area is impressive, reaching approximately 220,000 cm^2/g (according to the Blaine method). This exceptional characteristic gives it the ability to trap and fix calcium hydrate ($Ca(OH)$) while transforming it, initially, into hydrated silicate, and subsequently into stable and irreversible calcium silicate. This unique property has a significant impact on the behavior of concrete, both in the fresh and hardened states.

Fig 6. Silica Fume

Table 13. Technical and Chemical Characteristics of Silica Fume

Technical Data of Silica Fume	Physical State	Powder
	Color	Silver
	Particle Size	0,05 to 0,15 µm
	Density (g/cm^3 at 20°C)	Approximately 0,3
	Solubility in Water	Insoluble
Chemical Composition	SiO_2	> 95 %
	CaO	< 0,5 %
	MgO	< 1 %
	Fe_2O_3	< 1 %
	Ai_2O_3	< 0,5 %
	Other Components	Traces

2.3.2. *Admixture*

The admixture used is a superplasticizer based on new-generation polycarboxylates that enable the production of highly fluid concrete with very low water-to-cement ratios; see Table 14.

Table 14. Superplasticizer Characteristics

Appearance	Liquid
Color	Brown
Ph	5.5 ± 1
Density	1.13± 0.03
Na_2O Content	< 1%

2.4. *Formulation of concretes*

A total of eight concrete samples were prepared and labeled as follows: SCC00, SCC11, SCC12, SCC13, SCC21, SCC22, SCC23, and SCC31. Here, "i" represents the index of the additive, while "j" corresponds to the percentage of substitution of the additive in relation to the cement. The first formulation, SCC00, served as a reference and consisted of Self-Compacting Concrete (SCC) with the addition of limestone fillers. The other formulations involved variations in the amount of fillers, with proportions of 10%, 20%, and 30% of the white cement of class 52.5, as specified in

Table 15. The dosage of the superplasticizer was determined experimentally based on tests of fresh concrete, aiming to achieve a class SF1 spread.

Table 15. Concrete compositions of different types of Self-compacting concrete (SCC).

Constituents	Unité	SCC00	SCC11	SCC12	SCC13	SCC21	SCC22	SCC23	SCC31
Sand 0/1	[kg/m^3]	558	558	558	558	558	558	558	558
Sand 0/3	[kg/m^3]	235	235	235	235	235	235	235	235
Gravel 3/8	[kg/m^3]	326	326	326	326	326	326	326	326
Gravel 8/15	[kg/m^3]	489	489	489	489	489	489	489	489
Ciment	[kg/m^3]	400	360	320	280	360	320	280	360
Limestone filler	[kg/m^3]	100	100	100	100	100	100	100	100
Substitution P	[%]		10	20	30				
Pozzolana	[kg/m^3]		40	80	120				
Substitution VC	[%]					10	20	30	
Calcined mud	[kg/m^3]					40	80	120	
Substitution FS	[%]								10
Silica fume	[kg/m^3]								40
Water	[l]	210	210	210	210	210	210	210	210
Admixture	[l]	8	8	8	8	8	8	8	8

3. Results and discussion

3.1. Fresh State Test Results

Figure 7 presents the slump test results for various self-compacting concrete formulations. These results highlight that the different concretes fall within the SF1 class according to specifications (AFGC, 2008; EFNARC, 2005), indicating a slump ranging from 55 to 65 cm without any signs of bleeding or segregation.

The reduction in the slump of SCC12, SCC13, SCC22, and SCC23 is directly attributed to the increased specific surface area of the additives, such as pozzolana or calcined mud. By increasing the proportion of these fine additives in the concrete mix, the total specific surface area of the particles increases. This rise in specific surface area influences the flow properties of the concrete, resulting in a decrease in slump and a modification of its behavior.

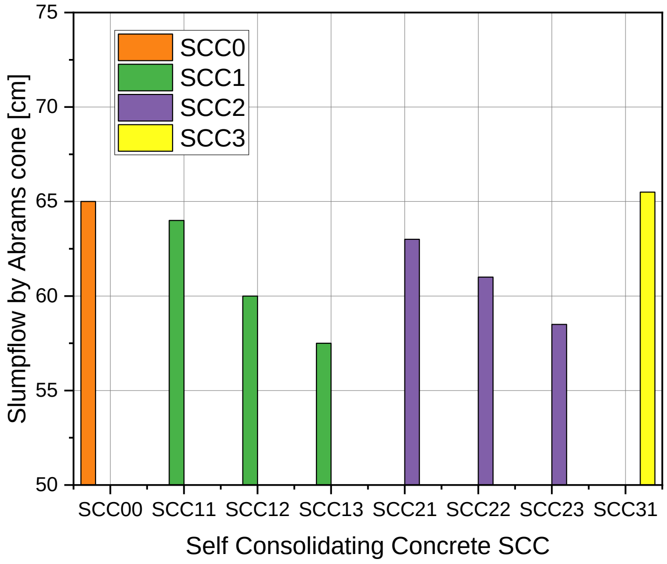

Fig 7. Slump flow by Abrams cone of Self-consolidating concrete mixtures.

Figure 8 presents the results of the L-box test for various self-compacting concrete formulations. These results highlight that the different concretes fall within the PA1 class according to specifications (AFGC, 2008; EFNARC, 2005), indicating a passing ability greater than a ratio of h2/h1 > 0.80.

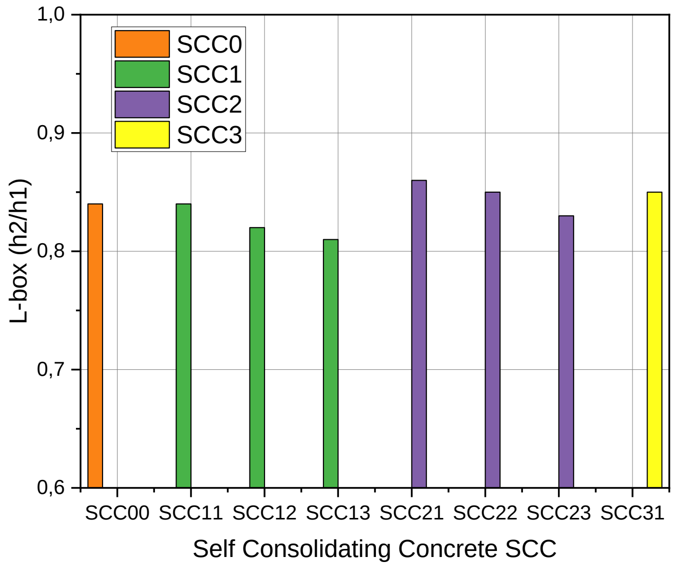

Fig 8. L-box (h2/h1) of Self-consolidating concrete mixtures.

Figure 9 presents the results of static segregation for various self-compacting concrete formulations. The sieve stability test results demonstrate that the tested compositions exhibit satisfactory stability, i.e., less than 15%, corresponding to an SR2 class (AFGC, 2008; EFNARC, 2005).

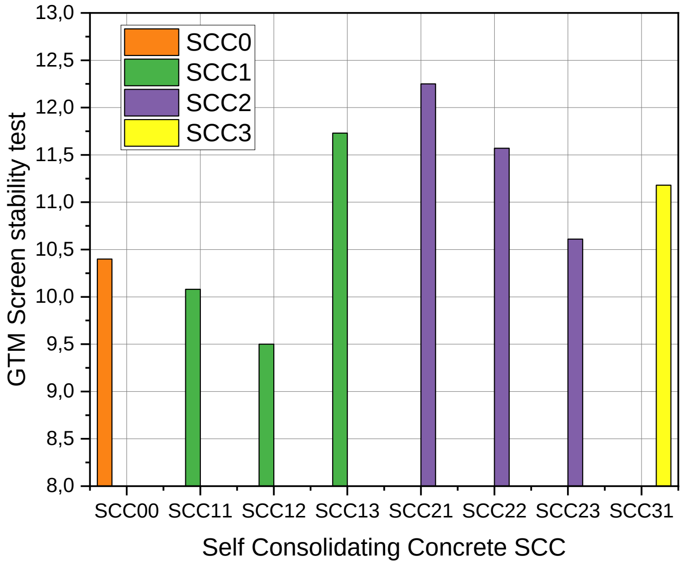

Fig 9. GTM Screen stability test of Self-consolidating concrete mixtures.

3.2. *Results of Hardened State Tests*

Figure 10 illustrates the evolution of the self-compacting concrete's compressive strength concerning the reference concrete, along with various substitutions of additives at different maturation stages. The compressive strength of all self-compacting concretes follows a similar kinetics. With the addition of 10% silica fume (SCC31), there is a 20% difference in favor of the reference self-compacting concrete SCC00 compared to pozzolanic additions and calcined clay additions up to 90 days. This difference can be explained by the dilution phenomenon, which is inversely proportional to the substitution rate. The higher the rate, the less cement is present, thus reducing the formation of hydrates (Safer et al., 2017).

The reference self-compacting concrete SCC13, with 30% pozzolanic substitution, shows a compressive strength approximately 40% lower compared to the reference mix SCC00 at 90 days. Similarly, a mix with a 30% substitution rate for SCC23, including calcined clay additives, exhibited a compressive strength about 15% lower.

The self-compacting concrete SCC11, with a 10% substitution of calcined clay, achieved a compressive strength of around 45 MPa at 90 days. The other concretes, with substitution rates of 20% and 30% for calcined clay, also showed very satisfactory results, reaching 33 MPa and 90 MPa, respectively (Frar et al., 2014; Safer et al., 2017).

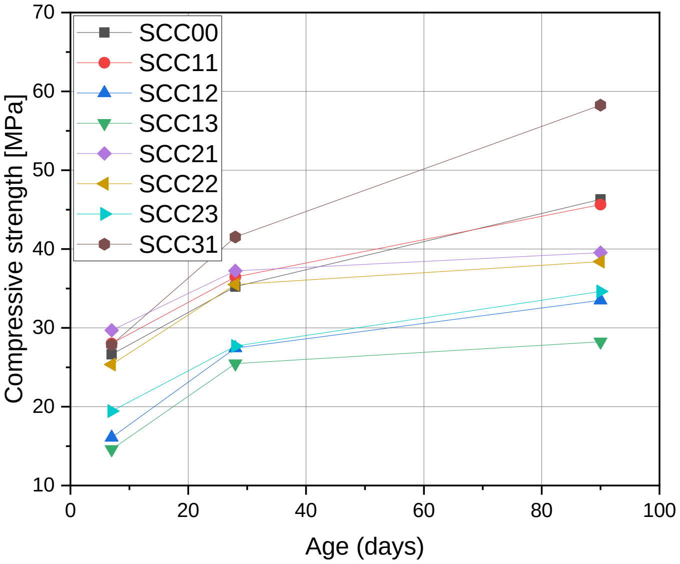

Fig 10. Compressive strengths of concretes in MPa, as a function of time.

Figure 11 illustrates the evolution of non-destructive ultrasonic tests concerning age compared to the reference concrete, along with various substitutions of additives at different maturation stages. Ultrasonic tests for all self-compacting concretes follow a similar trend. The results demonstrated that all concretes exhibit very high granular compactness, resulting in values exceeding 4500 at 28 days and 4600 at 90 days. With the addition of 10% for the reference concrete SCC11, SCC21, and SCC31, there is a negligible difference of less than 1% in favor of the reference self-compacting concrete SCC00 at 7 days. For the reference concrete SCC00, this difference is almost similar to that of the reference concrete SCC31, which incorporates silica fume, while other additives (SCC11 and SCC21) show a difference of 1%. With the addition of 10% for the reference concrete SCC11, SCC21, and SCC31, a negligible difference of less than 2% in favor of the reference self-compacting concrete SCC00 is observed at 90 days.

On the other hand, it is evident that increasing the amount of powder leads to a decrease in ultrasonic results for pozzolanic and calcined clay self-compacting concrete. This suggests that the powder absorbs mixing water and, after cement hydration, creates voids in the concrete, thereby reducing granular compactness.

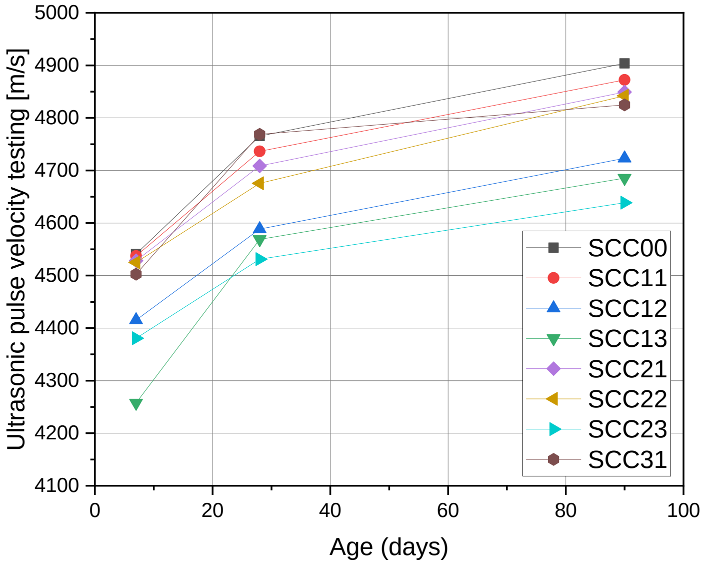

Fig 11. Ultrasonic pulse velocity testing as a function of time.

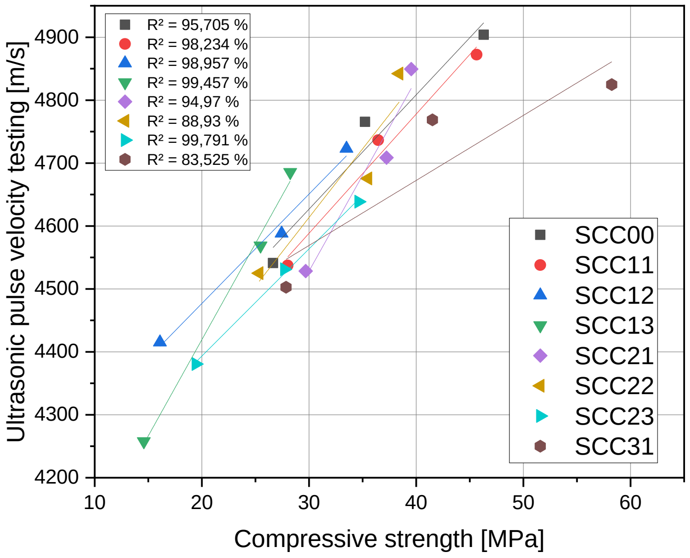

Fig 12. Correlation Between Compressive Strengths of Concretes and Ultrasonic Pulse Velocity Testing.

Figure 12 highlights the relationship between the results of compressive tests and ultrasonic tests (Ultrasonic Pulse Velocity Testing) concerning the reference concrete, along with various substitutions of additives at various maturation stages. The correlation analysis revealed an equation with a minimal coefficient of determination (R^2) of 83.525%. This high R^2 value indicates a significant correlation between non-destructive and destructive tests, revealing several relevant relationships between these two variables.

Using the data correlation, a trend curve was constructed, expressed by a linear equation, with a minimal coefficient of determination R^2 of 83.525%. This mathematical equation establishes a quantifiable relationship between non-destructive and destructive tests, providing the possibility to precisely quantify and predict how these two variables evolve together.

4. Conclusions

In conclusion, this study demonstrated the feasibility of valorizing reservoir dredging residues as a partial substitute for cement in concrete production. This approach provides an effective solution to the storage issue of dredging residues while contributing to enhanced environmental preservation and economic growth. The reuse of dredging residues transforms them from waste into a resource in line with sustainable development principles.

In the context of our research, we utilized calcined sludge, obtained at 850°C, to create a material with pozzolanic properties, referred to as artificial pozzolan. This calcined sludge was incorporated into self-compacting concrete as a partial replacement for class 52.5 white cement, at rates of 10%, 20%, and 30%, over periods of 7, 28, and 90 days.

To assess the performance of calcined sludge compared to natural pozzolan, a series of tests were conducted in both the fresh and hardened states. The results of these tests revealed that calcined sludge exhibits pozzolanic properties similar to those of natural pozzolan, with a spread ranging from 57.5 cm to 65.5 cm, fill rates exceeding 80% (0.81-0.86) for the L-box, and satisfactory stability of the tested concretes ($0 \leq \pi \leq 15\%$).

The correlation between the results of compressive strength tests and ultrasonic tests was demonstrated. Furthermore, the correlation between compressive strength test results and water content allowed the development of an equation introducing a new potential parameter in determining granular compactness through the compressive strength of self-compacting concrete, with a minimum coefficient of determination (R^2) of 88.525%.

5. References

AFGC. (2008). Recommandations pour l’emploi des bétons auto-plaçants. In *Association Française de Génie Civil*.

Benasla, M., Benamara, L., & Hadjel, M. (2015a). Caractérisation de la vase de dragage du barrage de l’Oued Fodda et valorisation en tant que matériau de construction (Characterization of dredging mud dam Oued Fodda and valorization as a building material). *J. Mater. Environ. Sci*, *6*(2), 546–558.

Benasla, M., Benamara, L., & Hadjel, M. (2015b). Characterization of dredging mud dam Oued Fodda and valorization as a building material. *J. Mater. Environ. Sci*, *6*(2), 546–558.

Bensafia, D., & Remini, B. (2016). Envasement Des Barrages Dans Les Regions Arides Exemples Algeriens Siltation of Dams in Arid Regions Algerian Examples. *Larhyss Journal*, *27*, 63–90.

De Gregorio, E., Occhicone, A., Montagnaro, F., Roviello, G., Ricciotti, L., & Ferone, C. (2023). A novel method of iron oxalate production through the valorization of red mud. *Chemical Engineering Research and Design*, *194*, 95–104. https://doi.org/10.1016/j.cherd.2023.04.036

EFNARC. (2005). The European Guidelines for Self-Compacting Concrete. In *The European Guidelines for Self Compacting Concrete* (Issue May).

Frar, I., Allal, L. Ben, Ammari, M., & Azmani, A. (2014). Utilisation des sédiments de dragage portuaire comme matière première dans la fabrication des briques en terre cuite. *Journal of Materials and Environmental Science*, *5*(2), 390–399.

Gázquez, M. J., Mantero, J., Bolívar, J. P., García-Tenorio, R., Vaca, F., & Lozano, R. L. (2011). Physico-chemical and radioactive characterization of TiO2 undissolved mud for its valorization. *Journal of Hazardous Materials*, *191*(1–3), 269–276. https://doi.org/10.1016/j.jhazmat.2011.04.075

Junakova, N., & Junak, J. (2017). Recycling of Reservoir Sediment Material as a Binder in Concrete. *Procedia Engineering*, *180*, 1292–1297. https://doi.org/10.1016/j.proeng.2017.04.291

Labiod, Z., Remini, B., & Belaredj, M. (2004). Traitement de la vase du barrage de bouhanifia en vue de sa valorisation. *Recherche*, 7–12.

Laoufi, L., Senhadji, Y., & Benazzouk, A. (2016). Valorization of mud from Fergoug dam in manufacturing mortars. *Case Studies in Construction Materials*, *5*, 26–38. https://doi.org/10.1016/j.cscm.2016.06.002

Li, Q., Wei, G., Duan, G., Zhang, L., Li, Z., & Yan, F. (2022). Valorization of ball-milled waste red mud into heterogeneous catalyst as effective peroxymonosulfate activator for tetracycline hydrochloride degradation. *Journal of Environmental Management*, *324*(August), 116301. https://doi.org/10.1016/j.jenvman.2022.116301

Mezencevova, A., Yeboah, N. N., Burns, S. E., Kahn, L. F., & Kurtis, K. E. (2012). Utilization of Savannah Harbor river sediment as the primary raw material in production of fired brick. *Journal of Environmental Management*, *113*, 128–136. https://doi.org/10.1016/j.jenvman.2012.08.030

Mohammed Krachaï, R., & Bouabdallah, M. A. (2020). Influence of segregation on the performance of self-compacting concrete in the fresh and hardened states. *Journal of Building Materials and Structures*, *7*(2), 178–187. https://doi.org/10.34118/jbms.v7i2.768

Remimi, B., & Hallouche, W. (2005). Previson De L ' Envasement Dans Les Barrages Du Maghreb. *Evolution*, *2002*, 69–80.

Remini, B. (2006). Valorisation de la vase des barrages quelques exemples algeriens. *Recherche*, 75–89.

Rodríguez, O., Kacimi, L., López-Delgado, A., Frías, M., & Guerrero, A. (2013). Characterization of Algerian reservoir sludges for use as active additions in cement: New pozzolans for eco-cement manufacture. *Construction and Building Materials*, *40*, 275–279. https://doi.org/10.1016/j.conbuildmat.2012.10.016

Safer, O., Belas, N., Belaribi, O., Belguesmia, K., Mebrouki, A., & Hamadache, M. (2017). Study of the behavior in the fresh and hardened state of an eco-concrete based on dredged sediments. *Journal of Materials and Environmental Science*, *8*(6), 2026–2033.